

# Using an Organic Molecule with Low Triplet Energy as a Host in a Highly Efficient Blue Electrophosphorescent Device\*\*

Cong Fan, Liping Zhu, Tengxiao Liu, Bei Jiang, Dongge Ma,\* Jingui Qin, and Chuluo Yang\*

**Abstract:** To achieve high efficiencies in blue phosphorescent organic light-emitting diodes (PhOLEDs), the triplet energies ( $T_1$ ) of host materials are generally supposed to be higher than the blue phosphors. A small organic molecule with low singlet energy ( $S_1$ ) of 2.80 eV and triplet energy of 2.71 eV can be used as the host material for the blue phosphor, [bis(4,6-difluorophenyl)pyridinato- $N,C^2$ ]iridium(III)] tetrakis(1-pyrazolyl)-borate (FIR6;  $T_1 = 2.73$  eV). In both the photo- and electro-excited processes, the energy transfer from the host material to FIR6 was found to be efficient. In a three organic-layer device, the maximum current efficiency of  $37 \text{ cd A}^{-1}$  and power efficiency of  $40 \text{ lm W}^{-1}$  were achieved for the FIR6-based blue PhOLEDs.

Owing to spin-orbit coupling, phosphorescent heavy-metal complexes can harvest both electro-generated singlet and triplet excitons in the emitting layer (EML) of PhOLEDs, achieving 100% internal quantum efficiency.<sup>[1]</sup> To avoid competitive de-excitation pathways, such as triplet-triplet annihilation and/or concentration quenching, the emissive phosphors as guests are generally dispersed into organic small-molecule or polymer host matrix, which play an indispensable role for energy transfer and charge transport.<sup>[2]</sup> To provide more balanced electron and hole fluxes in EML, bipolar host materials are currently drawn considerable attention.<sup>[3]</sup>

It is a challenge to design bipolar host materials for blue PhOLEDs. Apart from possessing hole- and electron-transporting mobility, it is universally believed that bipolar host materials for blue PhOLEDs should have higher triplet energies than the blue phosphors. Otherwise the energy of excitons located on the blue phosphors could exothermically transfer to the lower triplet states of host materials.<sup>[4]</sup> To

guarantee high triplet energies, wide band-gap bipolar host materials have been developed, such as bis[4-( $N$ -carbazolyl)-phenyl]phenylphosphine oxide (BCPO), 2,7-bis[diphenylphosphoryl]-9-[4-( $N,N$ -diphenylamino)phenyl]-9-phenylfluorene (POAPF), and 9-[3-(9H-carbazole-9-yl)phenyl]-3-(diphenylphosphoryl)-9H-carbazole (mCPPO1), which usually emit fluorescence in violet or ultraviolet region.<sup>[5]</sup> However, owing to their intrinsic low HOMO level and high LUMO level, simultaneously injecting holes and electrons into these wide band-gap bipolar host materials would be difficult, which could consequently bring about high drive voltages and low power efficiencies in the blue PhOLEDs.<sup>[6]</sup> Therefore, it is preferable to achieve a trade-off between the triplet energy and HOMO/LUMO level for host materials.

Recently, Padmaperuma et al. reported a high-efficiency sky-blue PhOLED hosted by a bipolar material with lower triplet energy than that of the sky-blue phosphor, [bis(4,6-difluorophenyl)pyridinato- $N,C^2$ ]iridium(III)] picolinate (FIRpic), providing that the adjacent hole- and electron-transporting materials possessed sufficiently high triplet energies to confine the triplet excitons in the emitting layer.<sup>[7]</sup> It would be of significance to see if this strategy could be applicable to the blue phosphor of FIR6.<sup>[8]</sup> Herein, we designed and synthesized a new host material, namely POBpMDPA, by integrating diarylamine and diphenylphosphine oxide into the biphenyl skeleton. The new host possesses close triplet energy (2.71 eV) to the blue phosphor of FIR6 (2.73 eV). Significantly, efficient energy transfer from the low triplet-state host material to the blue phosphor of FIR6 can be realized both in photo- and electro-excited processes. By employing FIR6 as the blue phosphor and the new compound as the host material, the blue PhOLEDs achieved a maximum current efficiency of  $34 \text{ cd A}^{-1}$ , a maximum power efficiency of  $34 \text{ lm W}^{-1}$ , and a maximum external quantum efficiency (EQE) of 18.1% with a good Commission International de l'Eclairage coordinate (CIE) of (0.15, 0.25).

Scheme 1 depicts the synthesis of the new compound, POBpMDPA. The intermediate of 2'-bromo- $N,N$ -di( $p$ -tolyl)-biphenyl-2-amine (BrBPMDPA) was obtained through the Suzuki coupling reaction of 2-(di- $p$ -tolylamino)phenylboronic acid with 1,2-dibromobenzene; BrBPMDPA then underwent lithiation, coupling with chlorodiphenylphosphine, and oxidation with hydrogen peroxide to afford the final product. All of the compounds were fully characterized by  $^1\text{H}$  NMR and  $^{13}\text{C}$  NMR spectrometry, mass spectrometry, and elemental analysis (see the Supporting Information). The molecular structure of POBpMDPA was further confirmed by the single-crystal X-ray diffraction analysis (Supporting Information, Figure S1). The compound showed good thermal stability as indicated by the decomposition temperature ( $T_d$ , correspond-

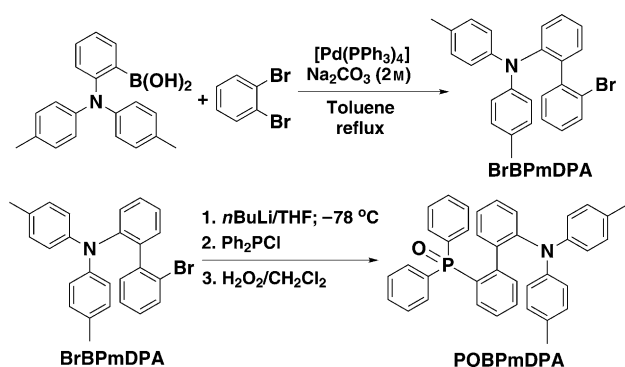
[\*] C. Fan,<sup>[†]</sup> T. Liu, B. Jiang, Prof. J. Qin, Prof. C. Yang  
Hubei Collaborative Innovation Center for Advanced Organic  
Chemical Materials, Hubei Key Lab on Organic and Polymeric  
Optoelectronic Materials, Department of Chemistry  
Wuhan University, Wuhan, 430072 (P.R. China)  
E-mail: clyang@whu.edu.cn

L. Zhu,<sup>[†]</sup> Prof. D. Ma  
State Key Laboratory of Polymer Physics and Chemistry  
Changchun Institute of Applied Chemistry  
Chinese Academy of Sciences, Changchun, 130022 (P.R. China)  
E-mail: mdg1014@ciac.jl.cn

[†] These authors contributed equally to this work.

[\*\*] We are grateful to the National Basic Research Program of China (973 Program 2013CB834805) and the National Science Fund for Distinguished Young Scholars of China (No. 51125013).

Supporting information for this article is available on the WWW under <http://dx.doi.org/10.1002/ange.201308046>.

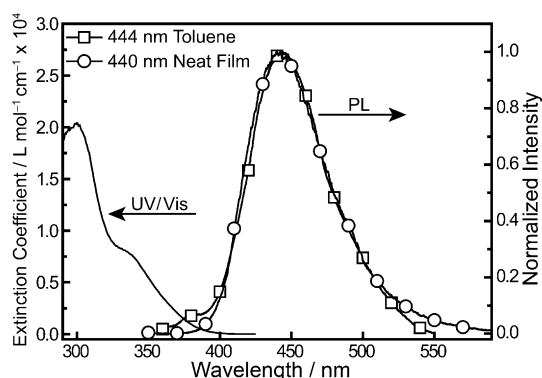


**Scheme 1.** Synthesis of POBPmDPA.

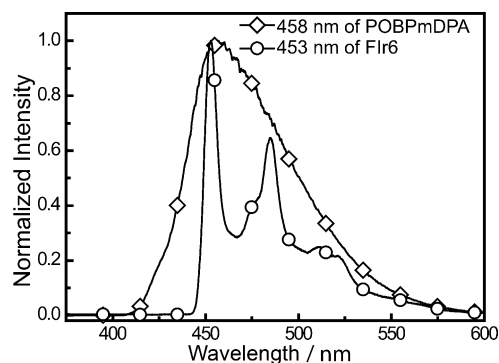
ing to 5% weight loss) of 296 °C (Supporting Information, Figure S2) and the glass transition temperature ( $T_g$ ) of 88 °C in the differential scanning calorimetry (DSC) thermogram (Supporting Information, Figure S2 inset). The electrochemical properties of POBPmDPA were probed by cyclic voltammetry (CV). It exhibited a reversible oxidation process in  $\text{CH}_2\text{Cl}_2$  solution with a half-wave oxidation potential ( $E_{\text{ox}}$  vs. ferrocene/ferricenium) of 0.36 V (Supporting Information, Figure S3), and accordingly, its HOMO energy was estimated to be  $-5.2$  eV, which was close to most triphenylamine derivatives.

Figure 1 shows the absorption spectrum of POBPmDPA in  $\text{CH}_2\text{Cl}_2$  solution and fluorescence (FL) spectra in toluene and neat film. The optical energy band gap ( $E_g$ ) of POBPmDPA was calculated to be 3.2 eV from the onset of absorption (388 nm). The fluorescence emission peaks of POBPmDPA were 444 nm in toluene solution and 440 nm in neat film; accordingly, its singlet state ( $S_1$ ) was estimated to be 2.80 eV. The phosphorescence spectrum of POBPmDPA in the 2-methyltetrahydrofuran (2-MeTHF) at 77 K (Figure 2) exhibited the highest-energy vibronic emission at 458 nm, from which the triplet energy ( $T_1$ ) of the compound was determined to be 2.71 eV. Under the same conditions, the triplet energy of FIr6 was estimated to be 2.73 eV.<sup>[8]</sup>

The new compound POBPmDPA possessed a nearly equal triplet energy to that of FIr6. To explore the nature of the photo-excited process between the host POBPmDPA and



**Figure 1.** UV/Vis absorption spectrum in  $\text{CH}_2\text{Cl}_2$  solution ( $10^{-5}$  M) and fluorescence spectra in toluene ( $\square$ ,  $10^{-5}$  M) and a neat film ( $\circ$ ) at room temperature.



**Figure 2.** Phosphorescence spectra of POBPmDPA and FIr6 in a 2-MeTHF matrix ( $10^{-5}$  M) at 77 K.

the dopant FIr6, we investigated the photoluminescence (PL) spectrum and lifetime of FIr6 doped in POBPmDPA matrix at 10% ratio by weight. For comparison, the PL spectrum and lifetime of FIr6 doped in polymethylmethacrylate (PMMA) matrix were also measured under the identical conditions. As Figure 3 showed, the emission of FIr6-POBPmDPA composite film predominantly originated from FIr6 molecule at both room temperature and 77 K, which is almost the same with the FIr6-PMMA composite film (Supporting Information, Figure S4). This is indicative of the efficient energy transfer from POBPmDPA to FIr6 in the photo-excited process. The

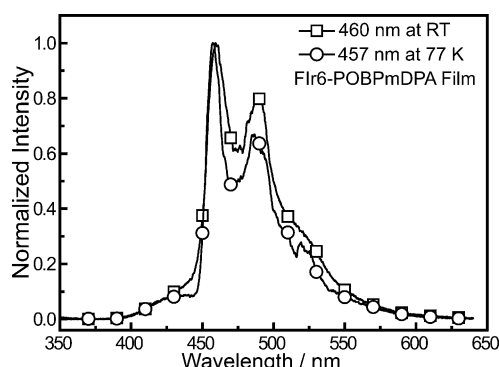


**Figure 3.** Photoluminescence spectra of FIr6-POBPmDPA composite film (10 wt%) at room temperature and 77 K (excitation at 330 nm).

PL intensity of FIr6 emission in FIr6-POBPmDPA composite film displayed almost monoexponential decay (7 ns (6%) and 2.2  $\mu\text{s}$  (94%); Supporting Information, Figure S5). The lifetime was nearly equal to that of FIr6 in FIr6-PMMA composite film at the same conditions. The lifetime domain of the FIr6-POBPmDPA composite film was assigned to FIr6 emission, indicating that the photo-excited excitons of FIr6 could not be quenched by the host POBPmDPA.

Though the compound POBPmDPA showed almost equal triplet energy to FIr6, the efficient energy transfer from POBPmDPA to FIr6 in the photo-excited process encouraged us to fabricate the FIr6-based PhOLEDs. We initially fabricated the blue device A with the following configuration: ITO/MoO<sub>3</sub> (10 nm)/TAPC (60 nm)/POBPmDPA:FIr6 (20 nm)/TmPyPB (35 nm)/LiF/Al. In device A, MoO<sub>3</sub> and

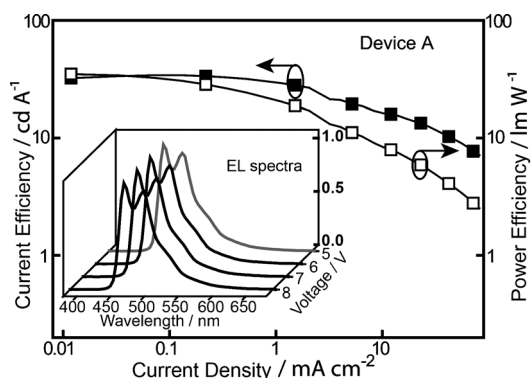


**Figure 4.** Current efficiency and power efficiency versus current density of device A (Inset: EL spectra at 5–8 V).

LiF served as the hole- and electron-injecting materials; FIr6 doped in POBpMDPA with optimized doping level of 10% was used as the emitting layer. TAPC [1,1-bis((di-4-tolylamino)phenyl)cyclohexane] and TmPyPB [1,3,5-tri(*m*-pyrid-3-ylphenyl)benzene] acted as the hole- and electron-transporting materials, respectively. It should be mentioned that TAPC and TmPyPB possess higher triplet energies (TAPC,  $T_1 = 2.87$  eV; TmPyPB,  $T_1 = 2.78$  eV) than that of FIr6 to confine the excitons in the EML.<sup>[9]</sup> The current efficiency and power efficiency versus current density of device A were shown in Figure 4. Remarkably, device A displayed rather high efficiencies with a maximum current efficiency of  $34 \text{ cd A}^{-1}$ , a maximum power efficiency of  $34 \text{ lm W}^{-1}$ , and a maximum EQE of 18.1%. At a practical brightness of  $100 \text{ cd m}^{-2}$  ( $0.35 \text{ mA cm}^{-2}$ , 3.9 V), device A still had a high current efficiency of  $33 \text{ cd A}^{-1}$ , power efficiency of  $26 \text{ lm W}^{-1}$ , and EQE of 17%. These efficiencies were comparable to the best results of FIr6-based devices summarized in Table 1. Moreover, these high efficiencies were acquired in a three organic-layer device structure, in contrast to those high-efficiency blue PhOLEDs required at least four organic layers.<sup>[5a,9a,10]</sup> It is also noteworthy that the electroluminescence (EL) of device A showed typical and stable FIr6 emission with good CIE

**Table 1:** Summary of some host materials for FIr6-based devices.

Host material	$S_1$ [eV] <sup>[a]</sup>	$T_1$ [eV] <sup>[b]</sup>	$CE_{\text{max}}$ [ $\text{cd A}^{-1}$ ] <sup>[c]</sup>	$PE_{\text{max}}$ [ $\text{lm W}^{-1}$ ] <sup>[d]</sup>	$EQE_{\text{max}}$ [%] <sup>[e]</sup>
BCPO <sup>[5a]</sup>	3.2	3.01	36.8	33.1	19.8
Ad-Pd <sup>[9b]</sup>	—	2.97	—	33	19
POBPCz <sup>[9c]</sup>	3.1	3.01	40	36	19.5
POBpMDPA (this work)	2.8	2.71	34	34	18.1

[a] Singlet state. [b] Triplet state. [c] Maximum current efficiency.

[d] Maximum power efficiency. [e] Maximum external quantum efficiency.

**Table 2:** Summary of devices A–C with the following device configuration: ITO/MoO<sub>3</sub> (10 nm)/HTL/POBpMDPA:FIr6 (20 nm)/ETL/LiF/Al.

Device	HTL	ETL	$V_{\text{on}}$ <sup>[a]</sup>	$CE_{\text{max}}$ <sup>[b]</sup>	$PE_{\text{max}}$ <sup>[c]</sup>	$EQE_{\text{max}}$ <sup>[d]</sup>	CIE (x, y) <sup>[e]</sup>
A	TAPC ( $T_1 = 2.87$ eV) (60 nm)	TmPyPB ( $T_1 = 2.78$ eV) (35 nm)	2.9 V	$34 \text{ cd A}^{-1}$	$34 \text{ lm W}^{-1}$	18.1%	(0.15, 0.25)
B	NPB ( $T_1 = 2.41$ eV) (70 nm)	TmPyPB ( $T_1 = 2.78$ eV) (35 nm)	2.9 V	$37 \text{ cd A}^{-1}$	$40 \text{ lm W}^{-1}$	17.9%	(0.16, 0.30)
C	TAPC ( $T_1 = 2.87$ eV) (60 nm)	BCP ( $T_1 = 2.5$ eV) (35 nm)	3.3 V	$9 \text{ cd A}^{-1}$	$7 \text{ lm W}^{-1}$	5.3%	(0.15, 0.23)

[a] Turn-on voltages at  $1 \text{ cd m}^{-2}$ . [b] Maximum current efficiency. [c] Maximum power efficiency. [d] Maximum external quantum efficiency. [e] CIE coordinates at 6 V.

coordinates of (0.15, 0.25) during operational voltages of 5–8 V (inset of Figure 4).

To study the influence of adjacent hole- and electron-transporting materials on the FIr6-based PhOLEDs, we further fabricated devices B and C. Compared to device A, NPB (1,4-bis(1-naphthylphenylamino)-biphenyl) with a low triplet energy of 2.41 eV was used to replace TAPC as the hole-transporting material in device B, whereas BCP (2,9-dimethyl-4,7-diphenyl-1,10-phenanthroline) with a low triplet energy of 2.50 eV was used to replace TmPyPB as the electron-transporting material in device C.<sup>[11]</sup> The current efficiency, power efficiency versus current density along with EL spectra of devices B and C are shown in the Supporting Information, Figure S7, and all the data are collected in Table 2. Usually, lower triplet-energy hole-/electron-transporting materials than that of phosphor could not block the diffusion of triplet excitons from EML. This may result in the change of EL spectrum or the decreased device efficiency.<sup>[12]</sup> Devices B and C, which use low triplet-energy hole- and electron-transporting materials, still displayed the typical EL spectra originated from FIr6 emission, with CIE coordinates of (0.16, 0.30) and (0.15, 0.23), respectively. This implied that the FIr6 excitons were well formed and manipulated inside the EML in devices B and C.

Furthermore, we also noted that device B exhibited high efficiencies with a maximum current efficiency of  $37 \text{ cd A}^{-1}$ , a maximum power efficiency of  $40 \text{ lm W}^{-1}$ , and a maximum EQE of 17.9%, which were comparable to those of device A. To the best of our knowledge, the device represented the highest power efficiency (PE) for FIr6-based blue PhOLEDs, and even higher than those of FIr6-based PhOLEDs with *n*-doped ETL ( $PE_{\text{max}}$  of  $39.2 \text{ lm W}^{-1}$ )<sup>[10a]</sup> or *p-i-n* structure ( $PE_{\text{max}}$  of  $36 \text{ lm W}^{-1}$ ).<sup>[10d]</sup> In contrast, device C showed fair efficiencies with a maximum current efficiency of  $9 \text{ cd A}^{-1}$ , a maximum power efficiency of  $7 \text{ lm W}^{-1}$ , and a maximum EQE of 5.3%. This suggested that the formed excitons in EML could be partially quenched by the low triplet energy of BCP in device C, whereas they could be hardly quenched by the low triplet energy of NPB in device B. We presumed that the exciton-recombination zone be near the interface between the EML and the ETL in devices. Why has this situation arisen? One factor is that the holes in device C could be accumulated in the interface between the EML and ETL owing to the poor electron mobility of BCP in comparison with TmPyPB in device A (electron mobility: BCP  $\approx 10^{-6} \text{ cm}^2 \text{ V}^{-1} \text{ s}^{-1}$  vs. TmPyPB  $\approx 10^{-3} \text{ cm}^2 \text{ V}^{-1} \text{ s}^{-1}$ ).<sup>[13]</sup> Another factor was that the host material POBpMDPA may have significantly higher hole mobility than its electron mobility.

To confirm the hypothesis, we investigated the electron-/hole-transporting characters of POBpMDPA by fabricating

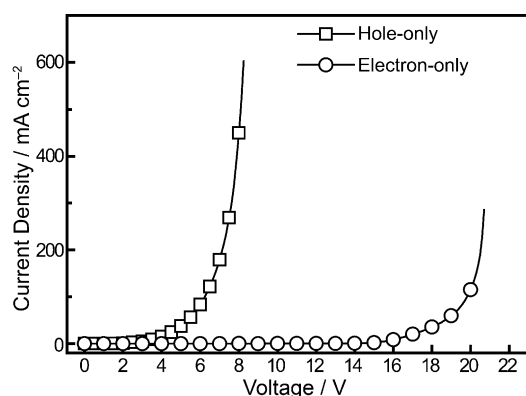


**Figure 5.** Current density versus voltage of the hole- and electron-only devices.

the hole-only device with the structure: ITO/MoO<sub>3</sub> (10 nm)/TAPC (10 nm)/POBPmDPA (30 nm)/TAPC (10 nm)/MoO<sub>3</sub> (10 nm)/Al, and the electron-only device with the structure: ITO/LiF (1 nm)/TmPyPB (10 nm)/POBPmDPA (30 nm)/TmPyPB (10 nm)/LiF (1 nm)/Al. In the two devices, MoO<sub>3</sub> and LiF served as the hole- and electron-injecting materials; TAPC and TmPyPB were used to prevent electron and hole injecting from the cathode and anode, respectively. As depicted in the current density versus voltage curve (Figure 5), the hole-only device exhibited substantially higher current density than the electron-only device under the same voltage, manifesting the dominating hole-transporting ability of POBPmDPA.

In conclusion, our research has revealed that efficient energy transfer from a low singlet/triplet-state host material to the blue phosphor of FIr6 can be realized both in photo- and electro-excited processes. Providing that hole- and electron-transporting materials with high triplet energies and good carrier mobilities were used, highly efficient blue PhOLEDs with the maximum current efficiency of 34 cd A<sup>-1</sup> and power efficiency of 34 Lm W<sup>-1</sup> were achieved, even though the triplet energy of host material was not higher than the blue phosphor. The encouraging results would bring down the threshold for designing host materials and open a new way for the development of blue PhOLEDs. The energy transfer process between the new host and guest in these blue PhOLEDs will be further investigated.

## Experimental Section

**PhOLED fabrication and measurement:** The hole-injecting material (MoO<sub>3</sub>), hole-transporting materials (NPB, TAPC), and electron-transporting materials (TmPyPB, BCP) are commercially available. Indium tin oxide (ITO)-coated glass with sheet resistance of 10 Ω square<sup>-1</sup> was used as the starting substrates. Before device fabrication, the ITO glass substrates were pre-cleaned carefully and treated by UV/O<sub>3</sub> for 2 min. Then the sample was transferred to the deposition system. MoO<sub>3</sub> was firstly deposited to ITO substrates, followed by HTL, the emissive layer, and ETL. Finally, a cathode composed of 1 nm of lithium fluoride and 120 nm of aluminum was sequentially deposited onto the substrates in the vacuum of 10<sup>-6</sup> Torr to construct the device. In the deposition of the emissive layer, the host and guest were placed into different evaporator sources. The

deposition rates of both host and guest were controlled with their correspondingly independent quartz crystal oscillators. The evaporation rates were monitored by a frequency counter and calibrated by a Dektak 6M profiler (Veeco). The current density–voltage–luminance of the device was measured with a Keithley 2400 Source meter and a Keithley 2000 Source multimeter equipped with a calibrated silicon photodiode. The EL spectra were measured by a JY SPEX CCD3000 spectrometer. All of the measurements were carried out at room temperature under ambient conditions.

Received: September 13, 2013

Revised: October 29, 2013

Published online: January 21, 2014

**Keywords:** blue phosphorescence · organic light-emitting diodes · triplet state

- [1] a) M. A. Baldo, D. F. O'Brien, Y. You, A. Shoustikov, M. E. Thompson, S. R. Forrest, *Nature* **1998**, 395, 151–154; b) L. Xiao, Z. Chen, B. Qu, J. Luo, S. Kong, Q. Gong, J. Kido, *Adv. Mater.* **2011**, 23, 926–952; c) Y. Tao, Q. Wang, C. Yang, Q. Wang, Z. Zhang, T. Zou, J. Qin, D. Ma, *Angew. Chem.* **2008**, 120, 8224–8227; *Angew. Chem. Int. Ed.* **2008**, 47, 8104–8107; d) Y. Tao, C. Yang, J. Qin, *Chem. Soc. Rev.* **2011**, 40, 2943–2970; e) S. Gong, Y. Chen, C. Yang, C. Zhong, J. Qin, D. Ma, *Adv. Mater.* **2010**, 22, 5370–5373; f) S. Gong, Q. Fu, Q. Wang, C. Yang, C. Zhong, J. Qin, D. Ma, *Adv. Mater.* **2011**, 23, 4956–4959.
- [2] a) M. A. Baldo, S. Lamansky, P. E. Burrows, M. E. Thompson, S. R. Forrest, *Appl. Phys. Lett.* **1999**, 75, 4–6; b) R. J. Holmes, B. W. D'Andrade, S. R. Forrest, X. Ren, J. Li, M. E. Thompson, *Appl. Phys. Lett.* **2003**, 83, 3818–3820.
- [3] A. Chaskar, H.-F. Chen, K.-T. Wong, *Adv. Mater.* **2011**, 23, 3876–3895.
- [4] a) M. A. Baldo, S. R. Forrest, *Phys. Rev. B* **2000**, 62, 10958–10966; b) H. Sasabe, J. Takamatsu, T. Motoyama, S. Watanabe, G. Wagenblast, N. Langer, O. Molt, E. Fuchs, C. Lennartz, J. Kido, *Adv. Mater.* **2010**, 22, 5003–5007; c) C. Adachi, R. C. Kwong, P. Djurovich, V. Adamovich, M. A. Baldo, M. E. Thompson, S. R. Forrest, *Appl. Phys. Lett.* **2001**, 79, 2082–2084; d) Y. Li, H. Wu, C.-S. Lam, Z. Chen, H. Wu, W.-Y. Wong, Y. Cao, *Org. Electron.* **2013**, 14, 1909–1915.
- [5] a) H.-H. Chou, C.-H. Cheng, *Adv. Mater.* **2010**, 22, 2468–2471; b) F.-M. Hsu, C.-H. Chien, C.-F. Shu, C.-H. Lai, C.-C. Hsieh, K.-W. Wang, P.-T. Chou, *Adv. Funct. Mater.* **2009**, 19, 2834–2843; c) S. O. Jeon, S. E. Jang, H. S. Son, J. Y. Lee, *Adv. Mater.* **2011**, 23, 1436–1441.
- [6] H. Liu, G. Cheng, D. Hu, F. Shen, Y. Lv, G. Sun, B. Yang, P. Lu, Y. Ma, *Adv. Funct. Mater.* **2012**, 22, 2830–2836.
- [7] J. S. Swensen, E. Polikarpov, A. V. Ruden, L. Wang, L. S. Sapochak, A. B. Padmaperuma, *Adv. Funct. Mater.* **2011**, 21, 3250–3258.
- [8] X. Ren, J. Li, R. J. Holmes, P. I. Djurovich, S. R. Forrest, M. E. Thompson, *Chem. Mater.* **2004**, 16, 4743–4747.
- [9] a) S. Su, T. Chiba, T. Takeda, J. Kido, *Adv. Mater.* **2008**, 20, 2125–2130; b) H. Fukagawa, N. Yokoyama, S. Irida, S. Tokito, *Adv. Mater.* **2010**, 22, 4775–4778; c) C. Fan, F. Zhao, P. Gan, S. Yang, T. Liu, C. Zhong, D. Ma, J. Qin, C. Yang, *Chem. Eur. J.* **2012**, 18, 5510–5514.
- [10] a) J. Lee, J.-I. Lee, J.-W. Lee, H. Y. Chu, *Org. Electron.* **2010**, 11, 1159–1164; b) J. Lee, J.-I. Lee, J. Y. Lee, H. Y. Chu, *Appl. Phys. Lett.* **2009**, 95, 253304; c) C.-A. Wu, H.-H. Chou, C.-H. Shih, F.-I. Wu, C.-H. Cheng, H.-L. Huang, T.-C. Chao, M.-R. Tseng, *J. Mater. Chem.* **2012**, 22, 17792–17799; d) S.-H. Eom, Y. Zheng, E. Wrzesniewski, J. Lee, N. Chopra, F. So, J. Xue, *Org. Electron.* **2009**, 10, 686–691.

- [11] a) P.-I. Shih, C.-H. Chien, C.-Y. Chuang, C.-F. Shu, C.-H. Yang, J.-H. Chen, Y. Chi, *J. Mater. Chem.* **2007**, *17*, 1692–1698; b) Q.-X. Tong, S.-L. Lai, M.-Y. Chan, K.-H. Lai, J.-X. Tang, H.-L. Kwong, C.-S. Lee, S.-T. Lee, *Chem. Mater.* **2007**, *19*, 5851–5855; c) W. Y. Hung, T. H. Ke, Y. T. Lin, C. C. Wu, T. H. Hung, T. C. Chao, K. T. Wong, C. I. Wu, *Appl. Phys. Lett.* **2006**, *88*, 064102; d) M. E. Kondakova, T. D. Pawlik, R. H. Young, D. J. Giesen, D. Y. Kondakov, C. T. Brown, J. C. Deaton, J. R. Lenhard, K. P. Klubek, *J. Appl. Phys.* **2008**, *104*, 094501.
- [12] a) M. Cocchi, D. Virgili, C. Sabatini, J. Kalinowski, *Chem. Phys. Lett.* **2006**, *421*, 351–355; b) D. Virgili, M. Cocchi, V. Fattori, C. Sabatini, J. Kalinowski, J. A. G. Williams, *Chem. Phys. Lett.* **2006**, *433*, 145–149; c) Y. Zheng, S.-H. Eom, N. Chopra, J. Lee, F. So, J. Xue, *Appl. Phys. Lett.* **2008**, *92*, 223301.
- [13] a) M. Ichikawa, J. Amagai, Y. Horiba, T. Koyama, Y. Taniguchi, *J. Appl. Phys.* **2003**, *94*, 7796–7800; b) L. Xiao, X. Xing, Z. Chen, B. Qu, H. Lan, Q. Gong, J. Kido, *Adv. Mater.* **2013**, *25*, 1323–1330.
-